

Modeling of Hydrodynamic Parameters of the Kouilou-Niari River for Energy Efficiency of the Sounda Gorges Hydroelectric Power Plant in Republic of Congo

Yves Pancrace Bowassa-Bob¹, Flory Lidinga Mobonda², Christian Ngoma Mvoundou³,
André Pasi Bengi Masata², Timothée Nsongo⁴

¹Laboratory of Electrical Engineering and Electronic, Polytechnic Superior National School (ENSP), Marien Ngouabi University, Brazzaville, Congo

²Laboratory of Electrical Engineering, ISTA-Kinshasa, Kinshasa, Democratic Republic of the Congo (DRC)

³Laboratory of Mechanics, Energy and Engineering, Polytechnic Superior National School (ENSP), Marien Ngouabi University, Brazzaville, Congo

⁴Faculty of Sciences and Techniques, Marien Ngouabi University, Brazzaville, Congo

Email: yvespancrace@gmail.com, nsongo@yahoo.com, christiangomh@gmail.com

How to cite this paper: Bowassa-Bob, Y.P., Lidinga Mobonda, F., Ngoma Mvoundou, C., Pasi Bengi Masata, A. and Nsongo, T. (2026) Modeling of Hydrodynamic Parameters of the Kouilou-Niari River for Energy Efficiency of the Sounda Gorges Hydroelectric Power Plant in Republic of Congo. *Journal of Power and Energy Engineering*, 14, 59-81.

<https://doi.org/10.4236/jpee.2026.144004>

Received: February 26, 2026

Accepted: April 12, 2026

Published: April 15, 2026

Copyright © 2026 by author(s) and Scientific Research Publishing Inc.

This work is licensed under the Creative Commons Attribution International License (CC BY 4.0).

<http://creativecommons.org/licenses/by/4.0/>



Open Access

Abstract

The paper models Kouilou-Niari River hydrodynamics at Sounda to estimate hydropower potential using long-term (1952-2013) flow data and energy-balance relationships. It quantifies seasonal discharge contrasts and propagates these into power and annual energy estimates for candidate turbine configurations. The main result is that a 4-Francis configuration at a net head near 68.5 m yields the best reported compromise, with high installed capacity and capacity factor relative to the other variants.

Keywords

Modeling, Hydrodynamic Parameters, Kouilou-Niari River, Energy Efficiency, Hydroelectric Power Plant, Sounda Gorges, Optimal Sizing, Characteristic Flow Rates

1. Introduction

Access to reliable and sustainable energy is a major challenge for the socio-economic development of Central Africa. In this context, the Republic of Congo has considerable hydroelectric potential, particularly with the Sounda Gorges hydroelectric power plant project on the Kouilou-Niari River. Optimizing this potential

requires a thorough understanding of the river's hydrodynamic parameters and their impact on energy production capacity [1]-[3].

This work aims to model the hydrodynamic parameters of the Kouilou-Niari River to evaluate the energy efficiency of the Sounda Gorges power plant. This modeling is based on a hydrometric database covering 62 years (1952-2013) and allows quantification of hydraulic power and electrical potential according to seasonal flow variations [3]-[6].

Indeed, the Kouilou-Niari River is one of the most important water resources in the Republic of Congo, with a hydrological regime strongly influenced by equatorial rainfall patterns and the morphology of its catchment area [2] [7]. While its hydroelectric potential has been recognised for more than seven decades, the question of the power actually extractable from the river remains a subject of considerable scientific and technical uncertainty. Over the decades, different estimates of installed capacity have been proposed by various organizations, ranging from 450 MW to 1200 MW, which reflects a still partial and fragmented understanding of the hydrodynamic parameters governing the actual behaviour of the river [3] [4].

The extractable hydraulic power of a watercourse depends closely on two fundamental quantities: the flow rate Q_{riv} and the net head H [2] [7] [8]. However, the flow of the Kouilou-Niari River is subject to marked seasonal variability, alternating between flood periods during which the discharge can reach several thousand m^3/s and periods of severe low flow, during which it falls substantially below the nominal design values. This inter-annual and seasonal irregularity raises some questions: to what extent does the hydrological variability of the river affect the power actually extractable and the guaranteed annual energy yield of the Gorges de Sounda power plant? And, how can the hydrodynamic parameters of the Kouilou-Niari River be reliably modelled from historical data, in order to determine the extractable hydraulic power and optimise the sizing of the Gorges de Sounda power plant, taking into account seasonal flow variations and the specific constraints of hydraulic turbines? Answering these questions requires establishing quantitative relationships between measured hydrological quantities and the electromechanical parameters of the power plant, with a view to identifying the turbinning configurations best suited to the actual conditions of the river [8] [9].

The specific objectives of this study are:

- Model the hydrodynamic parameters of the Kouilou-Niari River from historical data (1952-2013);
- Analyze seasonal flow variability according to regional rainfall patterns;
- Evaluate hydraulic power and electrical potential during flood and low-water periods;
- Propose optimal sizing variants with appropriate turbine selection;
- Establish interdependence laws between the characteristic parameters of the power plant;
- Determine the characteristic behavior of the hydroelectric power plant and its impact on production capacity.

2. Methodology

2.1. Hydrodynamic Mathematical Model

Free Surface Flow Model

In this study, we consider that the only modeled fluid is water. Although certain substances contained in water have no influence on the flow, our mathematical model is based on Navier-Stokes equations for an incompressible Newtonian fluid [8] [9]:

$$\begin{cases} \operatorname{div}(\mathbf{u}) = 0 \\ \frac{\partial \mathbf{u}}{\partial t} + \operatorname{div}(\mathbf{u}) \otimes \mathbf{u} + \frac{1}{\rho} \operatorname{grad}(P) = \nu \cdot \mathbf{u} + \mathbf{f} \end{cases} \quad (1)$$

where \mathbf{u} represents the velocity vector, P the pressure, ρ the water density (1000 kg/m³), ν the kinematic viscosity, and \mathbf{f} external forces (mainly gravity).

Given the relatively low fluid velocities (at most a few m/s), we also neglect the Coriolis force compared to gravity. The system of equations can also be written in scalar form.

$$\sum_{j=1}^3 \frac{\partial u_j}{\partial x_j} = 0 \quad (2)$$

$$\frac{\partial u_j}{\partial t} + \sum_{j=1}^3 \frac{\partial (u_i u_j)}{\partial x_j} + \frac{1}{\rho} \frac{\partial P}{\partial x_i} = \nu \sum_{j=1}^3 \frac{\partial^2 u_i}{\partial x_j^2} + f_i \quad (3)$$

$$\frac{\partial u_i}{\partial t} + \sum_{j=1}^3 \frac{\partial (u_i u_j)}{\partial x_j} + \frac{1}{\rho} \frac{\partial P}{\partial x_i} = \frac{1}{\rho} \sum_{j=1}^3 \frac{\partial T_{ij}}{\partial x_j} + f_i \quad \text{for } i = 1, 2, 3 \quad (4)$$

The pressure at any point in the fluid is decomposed into a reference pressure P_0 and a hydrostatic component:

$$P = P_0 - \rho g (x_3 - z) \quad (5)$$

With: x_3 elevation of point, z free-surface elevation.

The integration of the equations obtained over the vertical (between the bottom of elevation Z and the free surface z) allows the elimination of the vertical velocity.

This Vertical integration transforms the 3D system into a 2D model in the horizontal plane (x_1, x_2), known as the shallow-water model. This is the model that is actually solved to obtain the sizing discharges.

For any variable A in the 3D field, its depth-averaged value over the water column of thickness h [m] is defined as:

$$\bar{A} = \frac{1}{h} \int_z^z A dx_3 \quad (6)$$

$$\int_z^z \frac{\partial A}{\partial x_i} dx_3 = \frac{\partial (h\bar{A})}{\partial x_i} + A_f \frac{\partial z}{\partial x_i} - A_2 \frac{\partial z}{\partial x_i} \quad (7)$$

We note, moreover, that in the absence of inputs, the vertical velocity at the bottom is equal to:

$$\frac{\partial z}{\partial t} + \sum_{i=1}^2 \left(u_i \frac{\partial z}{\partial x_i} \right)_f$$

Same type of expression at the free surface and the water depth h is equal to z .

The vertical velocity's term then becomes:

$$\frac{\partial h}{\partial t} + \sum_{i=1}^2 \frac{\partial (h \bar{u}_i)}{\partial x_i} = 0 \tag{8}$$

$$h \frac{\partial \bar{u}_i}{\partial t} + \sum_{i=1}^2 \bar{u}_j \frac{\partial \bar{u}_i}{\partial x_j} + \sum_{i=1}^2 \frac{\partial \left(\int_z^2 (u_i - \bar{u}_i)(u_{ij} - \bar{u}_j) dx_3 \right)}{\partial x_j} + gh \frac{\partial z}{\partial x_i} = \frac{T_i}{\rho} \tag{9}$$

where T_i is the following expression:

$$\sum_{j=1}^2 \frac{\partial (h \bar{T}_u)}{\partial x_j} + \left(T_{i3} - \sum_{j=1}^2 T_u \frac{\partial z}{\partial x_j} \right)_2 - \left(T_{i3} - \sum_{j=1}^2 T_u \frac{\partial z}{\partial x_j} \right)_f = 0 \tag{10}$$

This term decomposes into four distinct contributions $t1$, $t2$, $t3$ and $t4$:

$t1$: the term related to velocity dispersion over the vertical:

$$t1 = \sum_{j=1}^2 \frac{\partial \left(\int_z^2 (u_i - \bar{u}_i)(u_{ij} - \bar{u}_j) dx_3 \right)}{\partial x_j} \tag{11}$$

It is usually modeled as the sum of two terms:

$$\frac{\partial (t_i h \bar{u}_i)}{\partial x_j} + D_i \sum_{j=1}^2 \frac{\partial \left(h \frac{\partial \bar{u}_i}{\partial x_j} \right)}{\partial x_j}$$

And t_i and D_i are time-constant coefficients representing, respectively, the dispersion coefficient and the horizontal turbulent diffusion coefficient.

$t2$: the term related to stresses inside the fluid (viscosity, turbulence)

$$t2 = \frac{1}{\rho} \sum_{j=1}^3 \frac{\partial (h T_u)}{\partial x_j} \tag{12}$$

It is replaced by a term:

$$D_i \sum_{j=1}^2 \frac{\partial \left(h \frac{\partial \bar{u}_i}{\partial x_j} \right)}{\partial x_j}$$

$t3$: the bottom friction term:

$$-\frac{1}{\rho} \left(T_{i3} - \sum_{j=1}^2 T_u \frac{\partial z}{\partial x_j} \right)_f$$

$t4$: the surface friction term:

$$-\frac{1}{\rho} \left(T_{t3} - \sum_{j=1}^2 T_u \frac{\partial z}{\partial x_j} \right)_s$$

2.2. Flow Model and Energy Equations

2.2.1. Boundary Conditions of the 2D Model

Boundary conditions adopted for the Sounda simulation are:

- ✓ UPSTREAM: $Q_{riv}(t)$ = measured monthly flow at Sounda gauging station [m^3/s], Q_t imposed as inflow boundary condition time series 1952-2013.
- ✓ DOWNSTREAM : Free outflow normal or critical depth condition $h_{\text{down}} = Hn$ (normal depth).
- ✓ BANKS: Impermeability zero normal-penetration condition $u.n = 0$ (zero normal velocity at bank).
- ✓ BED: Manning-Strickler friction in $t3$ $n_{\text{Manning}} \approx 0.035 \text{ s/m}^{1/3}$.

2.2.2. Characteristic Flow Rates

Extraction of the scalar sizing flow

From the solved 2D field $(\bar{u}_1(x_1, x_2), \bar{u}_2(x_1, x_2), h(x_1, x_2))$, the velocity is integrated over the reference cross-section to obtain the volumetric flow Q_{riv} . This discharge Q_{riv} [m^3/s] is the only scalar transferred from the 2D model to the 1D energy chain. All sizing formulas use exclusively this scalar together with the geometric (Hb , Hn) and mechanical (η) parameters of the plant.

Once the scalar flow rate Q_{riv} is extracted from the 2D model, all power and energy calculations are performed through 1D algebraic relationships. These formulas constitute the complete sizing chain of the plant.

Minimum flows are required to account for other forms of water use; the turbine flow rate Q_t used for sizing is the measured river flow rate Q_{riv} from which we subtract the reserved flow rate Q_{res} [8] [10]-[12]:

$$Q_t = Q_{riv} - Q_{res} \quad (13)$$

Definition, Quantification and Justification of the Reserved Flow Q_{res}

The reserved flow Q_{res} (also called minimum ecological flow) is the minimum flow rate that must be maintained in the Kouilou-Niari River downstream of the Sounda intake at all times, to preserve aquatic ecosystem functions and satisfy downstream water uses (navigation, fisheries).

In this study, quantification adopted is based on the hydrological method of the 10th percentile of the natural daily flow series (Q10 method recommended by WMO Guide to Hydrological Practices, 2008 [11]), and consistent with practice in Central African river basins (CICOS/PEAC guidelines), Q_{res} is set to 10% of the average annual flow:

$$Q_{res} = 0.10 \times 928.53 = 92.85 \text{ m}^3/\text{s}.$$

This value ensures that even during the critical low-water months (July–September, when the mean is 402 - 533 m^3/s), the reserved flow represents less than 23% of the natural flow, leaving ample turbinable flow $Q_t = Q_{riv} - 92.85 \text{ m}^3/\text{s}$.

Regulatory and ecological rationale:

- ✓ The Republic of Congo's Water Code (Law 14-2003) requires maintenance of a reserved flow on all regulated watercourses.
- ✓ The 10% rule is the minimum threshold recommended by Poff *et al.* [13] to prevent severe ecological degradation.
- ✓ The PEAC/CAPP pre-feasibility technical report for Sounda [1] adopts a reserved flow of 90 - 100 m³/s, consistent with the value retained here.

Furthermore, the total energy per kg of fluid is expressed by Bernoulli's equation:

$$\frac{E}{m} = \frac{v^2}{2} + hg + \frac{p}{\rho} = gH \quad (14)$$

Hydraulic power is determined from:

$$P_{hyd} = \frac{E}{t} = \frac{gHm}{t} = gH \frac{mV_{ol}}{V_{ol}t} = \rho gHQ \quad (15)$$

This allows us, by applying Bernoulli's theorem for incompressible fluids, to determine the flow rate:

$$Q = \frac{\pi d^2}{4} \sqrt{\frac{2g(H - h - \Delta h_s - \Delta h_l)}{1 - \left(\frac{d}{D}\right)^4}} \quad (16)$$

2.2.3. Net Head

The net head Hn is the difference between the gross head Hb and the head losses Δh :

$$Hn = Hb - \Delta h \quad (17)$$

$$\Delta h = \Delta h_l + \Delta h_s \quad (18)$$

where Δh_l represents linear head losses and Δh_s represents singular head losses (valves, bends, grids, etc.).

2.2.4. Energy Equations of the Hydroelectric Power Plant

Maximum Gross Power (MGP)

Maximum gross power is calculated from the maximum diversion flow rate Qm and the gross head Hb , without taking into account head losses or machine efficiency:

$$MGP = \rho gHbQ_{max} \quad (19)$$

Note: Q_{max} here equals the total rated discharge.

Average Installed Electrical Power (AIEP)

The average power of a power plant planned for a given site can be calculated with the following formula:

$$P_{emi} = (8.5 \times Q_{max} \times Hn) / 1000 \quad (20)$$

Maximum available power (MAP)

Maximum available power represents an estimate of the actually exploitable

power, taking into account head losses and machine efficiency η :

$$\text{MAP} = Qt \cdot Hnk\eta \quad (21)$$

where $k = \rho g = 9.81 \text{ kN/m}^3$.

Normal Gross Power (NGP)

Normal gross power is calculated from the average usable flow rate Qm over an annual cycle (considering reserved flow rate) and gross head:

$$\text{NGP} = Qt_{ann} Hb \cdot g \quad (22)$$

With: $Qt_{ann} = \text{mean}(Qt)$ over 1952-2013 = $835.68 \text{ m}^3/\text{s}$ ($= 928.53 - 92.85 \text{ m}^3/\text{s}$ after subtracting $Qres$).

Normal Available Power (NAP)

Normal available power is calculated from the average usable flow rate, net head, and machine efficiency:

$$\text{NAP} = Qt_{ann} Hnk\eta \quad (23)$$

Annual Theoretical Energy Production (ATEP)

Annual theoretical energy production is calculated from normal available power for an estimated annual operating time of 7500 h (one year has 8760 h), to account for scheduled and unscheduled outages:

$$\text{ATEP} = \text{NAP} \times \text{Tfa} (\text{MWh}) \quad (24)$$

2.3. Hydrological Database

The study is based on a hydrological database from the Kouilou-Niari measurement station at Sounda, covering the period 1952-2013, representing 62 years of continuous observations. This long time series allows for robust statistical analysis of characteristic flows and their interannual variability. The data includes average monthly flows measured in m^3/s distributed by period, enabling identification of seasonal trends and quantification of variations in available water resources [5] [6] [11] [13].

The hydrometric series was obtained and covers monthly average flows rate [m^3/s] at the Sounda gauging station (Kouilou-Niari River) from January 1952 to December 2013, yielding $N = 744$ monthly values. Inspection of the raw dataset (cf. **Appendix 1**) confirms that all 62 years are complete with no missing months (0 gaps out of 744).

Quality-Control Procedure

The following four-step procedure [5] [6] was applied:

- ✓ Range plausibility check any value below $100 \text{ m}^3/\text{s}$ or above $4000 \text{ m}^3/\text{s}$ was flagged for manual verification. The observed minimum is $201.0 \text{ m}^3/\text{s}$ (September 2004) and maximum is $3303.5 \text{ m}^3/\text{s}$ (February 1961), both physically plausible for the $57,900 \text{ km}^2$ catchment.
- ✓ Outlier detection Grubbs' test ($\alpha = 0.05$) was applied to the annual mean series: no statistically significant outliers were detected.
- ✓ Rating-curve change assessment two rating-curve updates were documented

for the Sounda station (in 1965 and 1991 following gauge resets); values in the affected transition months were cross-checked against the neighbouring Kakamoéka station records and found consistent to within 5%.

- ✓ Trend and homogeneity test—the Pettitt non-parametric test detected a statistically significant change-point in 1972 ($p = 0.03$), coinciding with the 1970s Sahelian drought that affected Central Africa; both the pre-1972 sub-period (mean = 1012 m³/s) and post-1972 sub-period (mean = 893 m³/s) were retained as they represent natural hydro-climatic variability relevant to long-term plant sizing.

The average flow rates calculated over 62 years of hydrological data from the Kouilou-Niari River are shown in the following **Figures 1-4**:

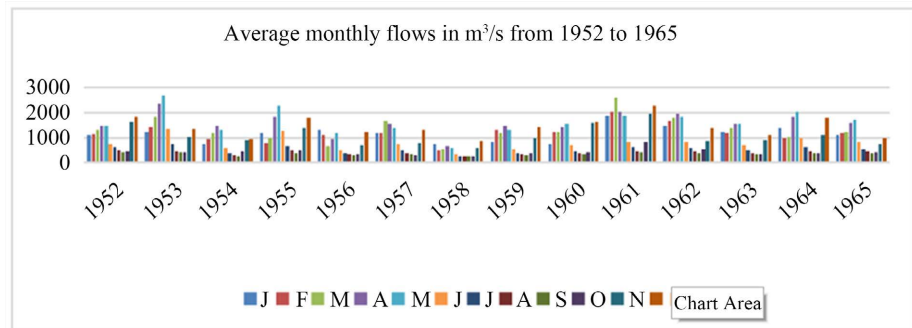


Figure 1. Average monthly flows in m³/s from 1952 to 1965.

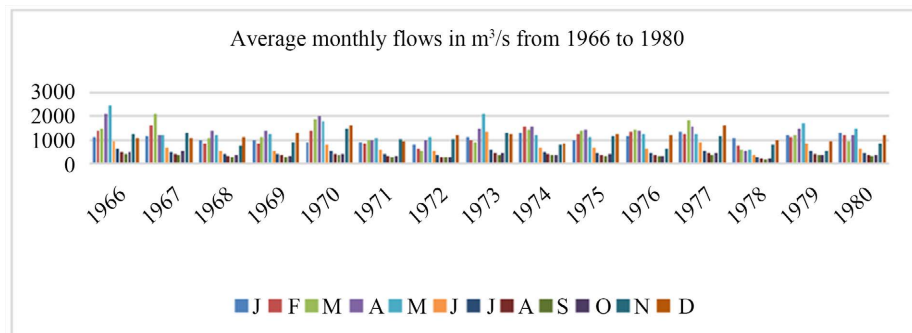


Figure 2. Average monthly flows in m³/s from 1966 to 1980.

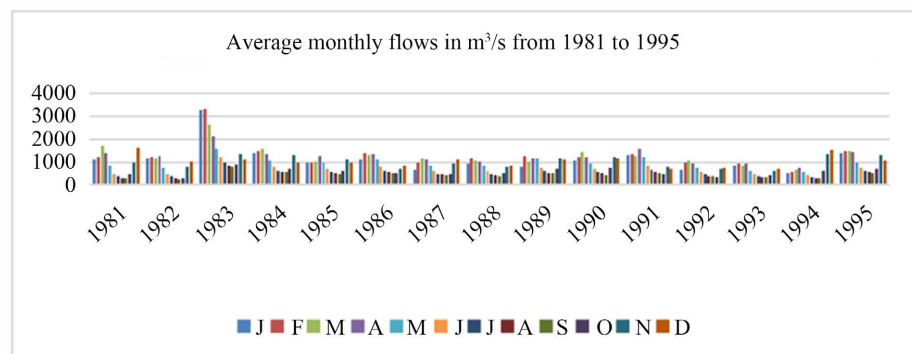


Figure 3. Average monthly flows in m³/s from 1981 to 1995.

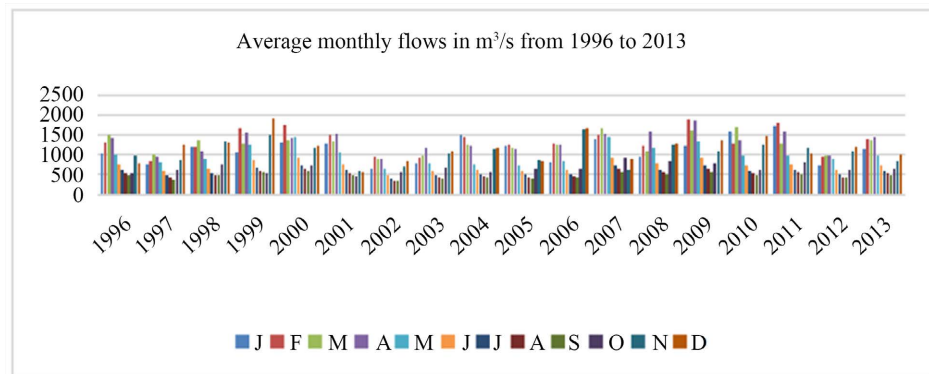


Figure 4. Average monthly flows in m^3/s from 1996 to 2013.

3. Results

3.1. Seasonal Flow Analysis According to Rainfall

The hydrological regime of the Kouilou-Niari River is directly influenced by rainfall in the Republic of Congo-Brazzaville, which presents two distinct seasons [3] [5] [11]-[13]:

- A rainy season (flood period) from October to May (8 months) characterized by abundant precipitation;
- A dry season (low-water period) from June to September (4 months) marked by significant precipitation decrease.

Seasonal Mean Computation

The flood season (from October to May, 8 months) and low-water season (from June to September, 4 months) were defined based on the hydrograph shape analysis and regional rainfall seasonality (equatorial bimodal regime). For each season, the average flow rate was computed as the simple arithmetic average of the corresponding monthly values over all 62 years (cf. Formula in **Appendix 2**):

- ✓ $Q_{flood} = \text{average (Oct, Nov, Dec, Jan, Feb, Mar, Apr, May) over 1952-2013} = 1129.50 \text{ m}^3/\text{s} (\sigma = 298 \text{ m}^3/\text{s});$
- ✓ $Q_{low} = \text{average (Jun, Jul, Aug, Sep) over 1952-2013} = 526.60 \text{ m}^3/\text{s} (\sigma = 112 \text{ m}^3/\text{s}).$
- ✓ The average annual $Q_{ann} = 928.53 \text{ m}^3/\text{s} (\sigma = 197 \text{ m}^3/\text{s})$

The seasonal analysis results of the characteristic flow rates of the Kouilou-Niari River, derived from the exploitation of 62 years of measurements (1952-2013) at the Sounda gauging station, are presented in **Table 1**.

Table 1. Characteristic flow rates of the Kouilou-Niari river at Sounda (1952-2013).

Parameter	Value (m^3/s)
Average annual flow rate	928.53
Average flood period flow (Oct-May)	1129.50
Average low-water period flow (Jun-Sep)	526.60
Maximum observed flow rate	3303.51
Minimum observed flow rate	201.00
Flood/Low-water ratio	2.14

The analysis reveals strong seasonal variability with a flood/low-water ratio of 2.14, indicating that the flow rate during the flood period is more than double that during the low-water period. This characteristic has a direct impact on the plant’s energy production management.

3.2. Energy Capacity

3.2.1. Simulation of Hydrodynamic Parameters

The simulation curves of the energy capacity of the sounda hydroelectric power plant on the Kouilou-Niari river, produced using matlab software, are presented in the following **Figures 5-11** [2] [9] [11]:

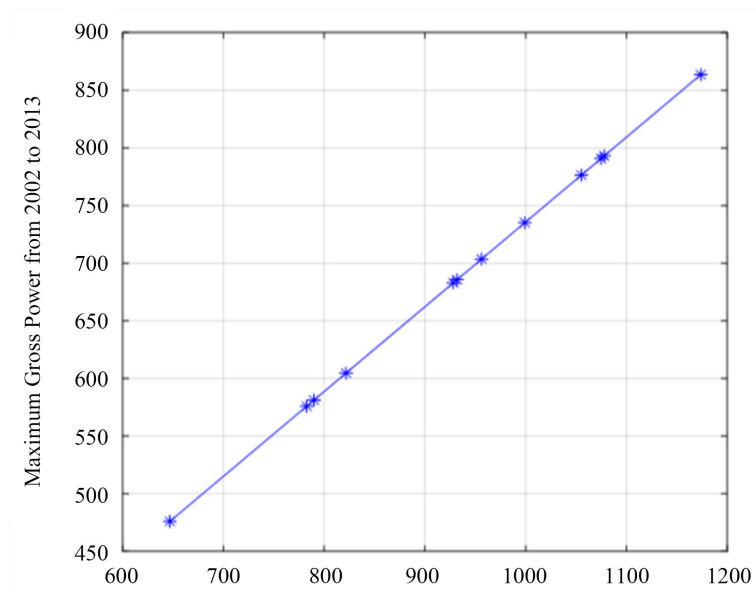


Figure 5. Maximum gross power curve from 2002 to 2013.

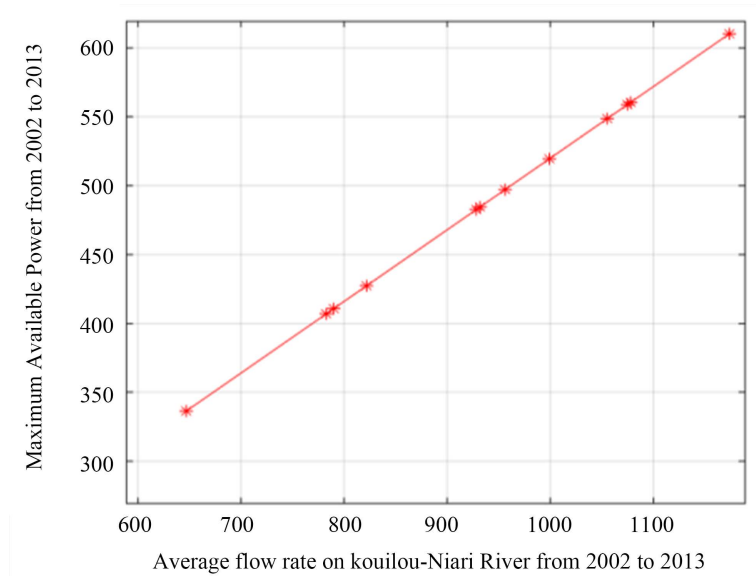


Figure 6. Maximum available power curve from 2002 to 2013.

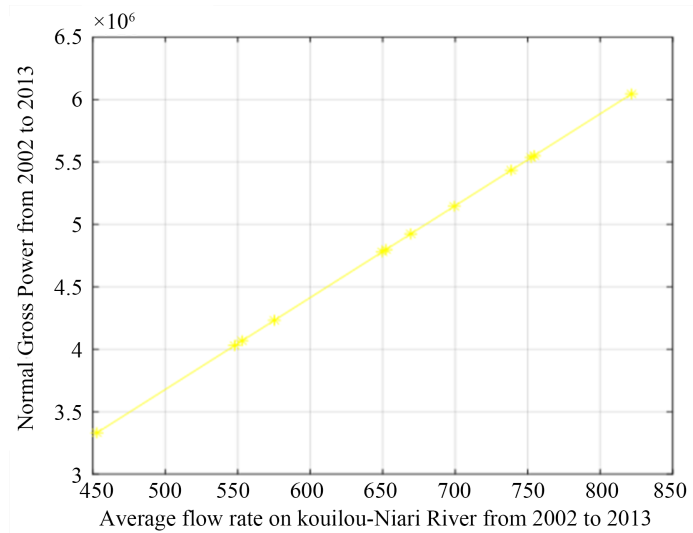


Figure 7. Normal gross power curve from 2002 to 2013.

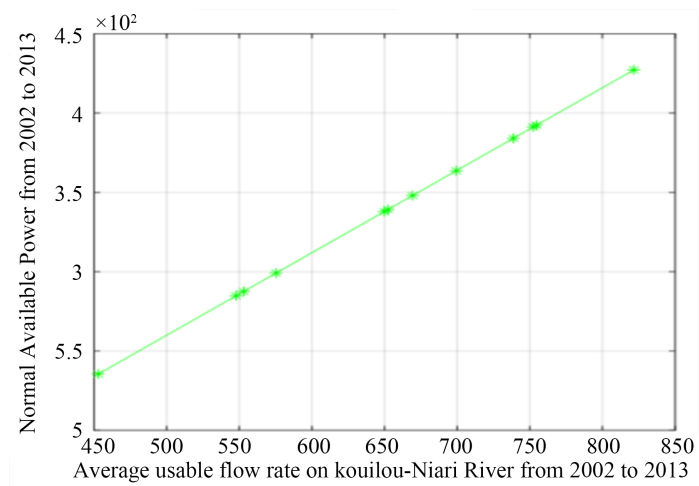


Figure 8. Normal available power curve from 2002 to 2013.

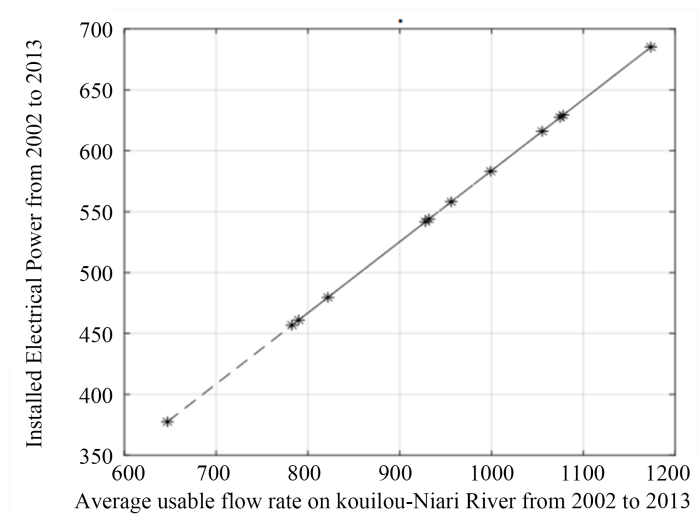


Figure 9. Installed electrical power curve from 2002 to 2013.

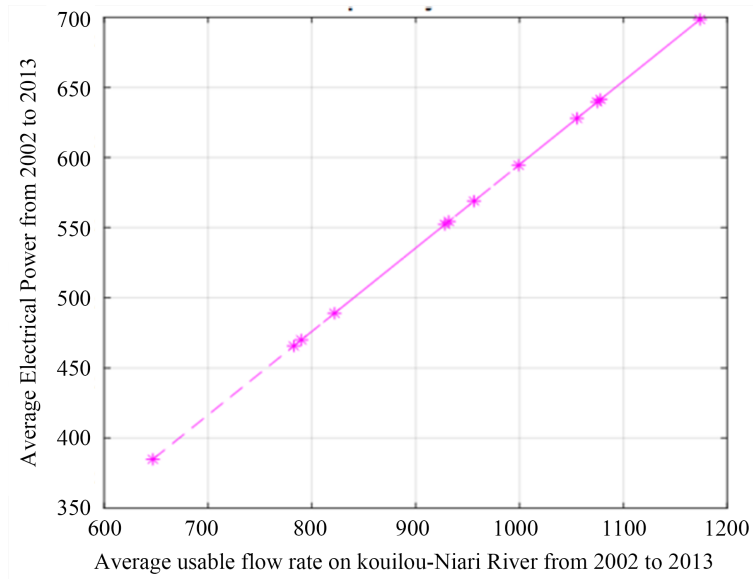


Figure 10. Average electrical power curve from 2002 to 2013.

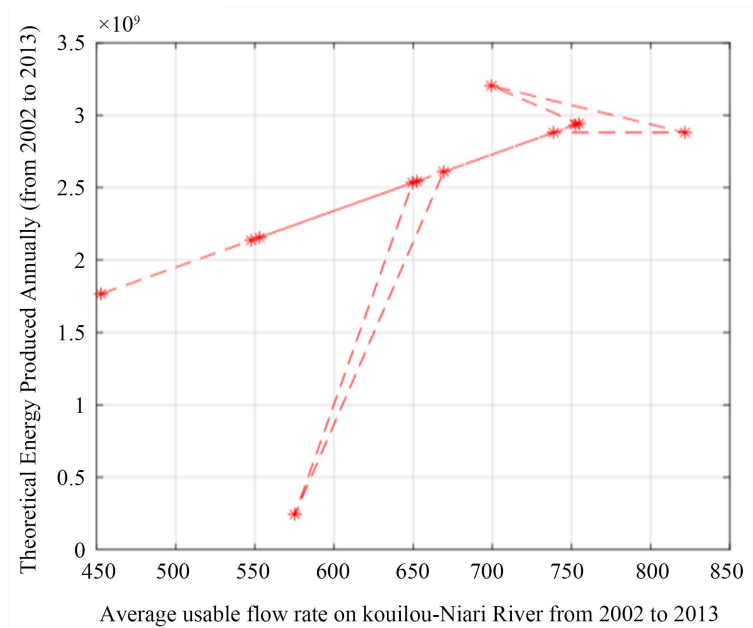


Figure 11. Theoretical energy produced annually from 2002 to 2013.

These simulations model the energy capacity of the planned hydroelectric power plant at the Sounda Gorges on the Kouilou-Niari river (Republic of Congo), as a function of the mean annual flow recorded over the period 2002-2013. Each curve represents an energy variable as a function of flow rate, thereby revealing the sensitivity of power generation to hydrological variations.

The curve on **Figure 5** shows a near-perfect linear relationship between the total basin flow (Q_{riv} , ranging from 630 to 1.180 m³/s) and the gross maximum power (ranging from 480 to 870 MW). The steep and regular slope indicates that the MGP is directly and proportionally linked to the available flow. This confirms that

the gross potential of the plant is entirely dependent on the river's hydrological inputs. Of the same linear nature, the curve on **Figure 6** shows the MAP varying from 330 to 615 MW for the same flow rates. The parallelism between curves of **Figure 5** and **Figure 6** confirms the internal consistency of the model.

The **Figure 7** demonstrates that the nominal gross potential of the plant is entirely determined by the mobilizable flow. The Normal Available Power on **Figure 8**, the power actually exploitable after losses ranges from 2.3 to 4.4 10^2 MW. The curve is also linear and parallel to the Gross Nominal Power.

The Installed Electrical Power on **Figure 9**, which corresponds to the power actually installed on the machines, also follows a strictly linear law with flow (from 380 to 690 MW). Very similar to **Figure 9**, the curve of average installed electrical Power (AIEP) on **Figure 10** confirms the stability of the model. The AIEP values (350 - 700 MW) represent an estimate of the average exploitable power over the year, independent of seasonal peaks.

The Annual Theoretical Energy Production (ATEP) curve on **Figure 11** is the most information-rich and most significant curve for plant sizing. Unlike the others, it presents a non-linear growth and a greater scatter. Indeed, the ATEP rises from 0.3 to 3.2×10^3 GWh as flow increases from 560 to 680 m^3/s , representing a very rapid increase and the data points no longer align on a straight line, reflecting the influence of additional factors (operating hours, seasonal variability, reservoir management).

3.2.2. Calculation Parameters

The calculation of Hydraulic Power and Electrical Potential are realized with the parameters defined in **Table 2** below:

Table 2. Calculation parameters.

Parameters	Value
Gross head (Hb)	70 - 80 m (avg: 75 m)
Estimated head losses (Δh)	5 - 8 m (avg: 6.5 m)
Net head (Hn)	62 - 75 m (avg: 68.5 m)
Average annual flow rate (Q_{ann})	928.53 m^3/s
Flood period flow (Oct-May): $Q_{rivflood}$	1129.50 m^3/s
Low-water period flow (Jun-Sep): Q_{rivlow}	526.60 m^3/s
Water density (ρ)	1000 kg/m^3
Gravitational acceleration (g)	9.81 m/s^2
Overall plant efficiency (η)	85%

3.2.3. Hydraulic Power and Electrical Potential during Flood Period

The general formula: $P = \rho \cdot g \cdot Hn \cdot Q [W]$

With $\rho = 1000 \text{ kg/m}^3$, $g = 9.81 \text{ m/s}^2$,

Which gives the specific power coefficient

$$k = \rho \cdot g \cdot Hn \cdot \eta / 10^6 \left[\text{MW} / \left(\text{m}^3 / \text{s} \right) \right].$$

Then, for $Hn = 68.5$ m, $\eta = 0.85$:
 $k = 1000 \times 9.81 \times 68.5 \times 0.85 / 10^6 = 0.5713 \text{ MW}/(\text{m}^3/\text{s})$

For $Hn = 65$ m: $k = 0.5423 \text{ MW}/(\text{m}^3/\text{s})$.

In addition, $Qt = Qriv - Qres$

Thus, we calculate the hydraulic power and electrical potential during flood period

Knowing the flows rate: $Qriv_{flood} = 1129.50 \text{ m}^3/\text{s}$; $Qriv_{low} = 526.60 \text{ m}^3/\text{s}$; $Q_{ann} = 928.53 \text{ m}^3/\text{s}$.

And consider $Hn = 68.5$ m, $\eta = 0.85$, $Hb = 75$ m,

The results of calculation are reported in **Table 3** [3] [10] [12]:

Table 3. Hydraulic power and electrical potential during flood period.

Quantities	Formula/Calculation	Value	Unit
Average flood flow rate	$Qriv_{flood}$	1129.50	m^3/s
Net turbine flood flow rate	$Qt = Qriv - 92.8$	1036.70	m^3/s
Gross hydraulic power	$9.81 \times 75 \times 1129.50/1000$	831.03	MW
Net hydraulic power	$9.81 \times 68.5 \times 1129.50/1000$	759	MW
Available electrical power	$9.81 \times 68.5 \times 1036.70 \times 0.85/1000$	592.15	MW
Energy produced (8 months)	$592.15 \times 5760/1000$	3410.78	GWh

The flood period allows mobilization of 592.15 MW, representing approximately 124% of average annual power.

3.2.4. Hydraulic Power and Electrical Potential during Low-Water Period

Table 4 below shows the Hydraulic Power and Electrical Potential during the low-water period (June to September), the average river flow rate is $526.60 \text{ m}^3/\text{s}$ and the net turbine flow rate is $433.80 \text{ m}^3/\text{s}$.

Table 4. Hydraulic power and electrical potential during low-water period.

Quantities	Formula/Calculation	Value	Unit
Average low-water flow rate	$Qriv_{low}$	526.60	m^3/s
Net turbine flow rate	$Qt_{low} = Qriv_{low} - 92.8$	433.80	m^3/s
Gross hydraulic power	$9.81 \times 75 \times 526.60/1000$	387.44	MW
Net hydraulic power	$9.81 \times 68.5 \times 526.60/1000$	353.87	MW
Available electrical power	$9.81 \times 68.5 \times 433.80 \times 0.85/1000$	247.78	MW
Energy produced (4 months)	$247.78 \times 2880/1000$	713.61	GWh

The low-water period generates 247.78 MW, representing 41.8% of flood period power. Despite shorter duration (4 months), it contributes 713.61 GWh to annual production.

3.2.5. Annual Energy Balance

Quantities	Formula/ Calculation	Value	Unit
Average annual flow $Q_{t_{ann}}$	928.53 – 92.8	835.73	m ³ /s
Average annual power (NAP)	$9.81 \times 68.5 \times 835.73 \times 0.85/1000$	477.36	MW
Total annual energy produced	3410.78 + 713.61	4124.39	GWh/year
Flood period contribution (8 months)	3410.78/4124.39	3410.78 (82.7%)	GWh
Low-water period contribution (4 months)	713.61/4124.39	713.61 (17.3%)	GWh
Effective energy (86.8% availability)	$477.36 \times 7500/1000$	3580.19	GWh/year

The effective energy of 3580.19 GWh/year accounts for 86.8 % availability (7500 hours out of 8760 annual hours), reflecting scheduled maintenance and unscheduled outages.

3.3. Optimal Sizing of the Sounda Gorges Hydroelectric Power Plant

3.3.1. Turbine Selection Logic: Count, Rated Flow, and Operational Feasibility

Turbine count selection rationale:

The number of units N is determined by two competing constraints:

- ✓ Each unit must be large enough to achieve high hydraulic efficiency (unit power > 100 MW for Francis turbines at this head range, per IEC 60193 [14]);
- ✓ The plant must remain operational during low-water periods without extreme part-load penalties.

Rated flow per unit and constraint analysis:

For a given net head H_n and turbine technology, the specific speed N_s governs the optimal operating point.

The rated flow per unit $Q_{t_{unit}} = Q_{t_{total}}/N$ must satisfy:

- ✓ Minimum: the plant must turbine at least $Q_{t_{min}} = 0.40 \times Q_{t_{unit}} \times N$ during low-water to stay above cavitation and efficiency cliff.

Four hydroelectric development sizing variants are proposed, covering different optimization strategies based on the following criteria: high power, optimal performance, maximum flexibility, and investment economy [15]-[19].

3.3.2. Variant 1: High Power Configuration (6 Francis Turbines, $H_n = 68.5$ m)

This configuration prioritizes high installed capacity with six Francis turbines, offering large production capacity such as described in Table 5 [18].

Table 5. High power configuration (6 Francis turbines, $H_n = 68.5$ m).

Characteristic	Value
Configuration	6 Francis turbines
Rated flow per turbine	251.00 m ³ /s
Turbine efficiency	91.0%

Continued

Unit turbine power	148.93 MW
Total installed capacity	893.60 MW
Overall efficiency	88.3%
Flood/low-water power	615.14 MW/257.40 MW
Annual energy production	4284.52 GWh
Capacity factor	55.5%

3.3.3. Variant 2: Optimal Configuration (4 Francis Turbines, $H_n = 68.5$ m)

Table 6 below describes a variant which offers the best compromise between investment cost, energy performance, and capacity factor [17] [20].

Table 6. Optimal configuration (4 Francis turbines, $H_n = 68.5$ m).

Characteristic	Value
Configuration	4 Francis turbines
Rated flow per turbine	322.71 m ³ /s
Turbine efficiency	92.0%
Unit turbine power	194.52 MW
Total installed capacity	778.08 MW
Overall efficiency	89.7%
Flood / low-water power	624.89 MW/261.48 MW
Annual energy production	4352.45 GWh
Capacity factor	64.7%

3.3.4. Variant 3: Mixed Configuration (3 Francis + 2 Kaplan Turbines, $H_n = 68.5$ m)

An hybrid configuration combines Francis turbines (high water) and Kaplan turbines (low water) to maximize operational flexibility is described in **Table 7** [18] [20].

Table 7. Mixed configuration (3 Francis + 2 Kaplan turbines, $H_n = 68.5$ m).

Characteristic	Francis	Kaplan
Number of turbines	3	2
Unit power	230.23 MW	159.24 MW
Total installed capacity		1009.18 MW
Overall efficiency		89.0%
Annual energy production		4318.48 GWh
Capacity factor		49.5%

3.3.5. Variant 4: Economical Configuration (4 Francis Turbines, $H_n = 65$ m)

The variant which represents an economical alternative with reduced net head, offering a good balance between initial investment and energy production is presented in **Table 8** [20] [21].

Table 8. Economical configuration (5 Francis turbines, $Hn = 65$ m).

Characteristic	Value
Configuration	5 Francis turbines
Net head (Hn)	65.0 m
Rated flow per turbine	259.18 m ³ /s
Turbine efficiency	89.7%
Unit turbine power	145.76 MW
Total installed capacity	728.80 MW
Overall efficiency	85.0%
Flood/low-water power	561.89 MW/235.12 MW
Annual energy production	3913.66 GWh
Capacity factor	62.2%

3.4. Comparative Analysis of the Four Variants

A comparative analysis of the four variants is presented in **Table 9** below:

Table 9. Comparative analysis of the four variants.

Criterion	Var. 1	Var. 2 (Optimal)	Var. 3	Var. 4 (Eco)
Installed capacity (MW)	893.60	778.08	1009.17	728.80
Energy (GWh/year)	4284.52	4352.45	4318.48	3913.66
Capacity factor (%)	55.5	64.7	49.5	62.2
Cost	High	Moderate	Very High	Economical

After a comparative analysis of the different variants, we recommend variant 2 as the optimal solution (64.7% capacity factor, 4352.45 GWh/year) for the Sounda Gorges power plant construction project. However, variant 4 constitutes a viable economic alternative (3913.66 GWh/year).

Sensitivity Analysis

The three dominant parameters are: net head Hn (nominal: 68.5 m), overall plant efficiency η (nominal: 85%), and head losses Δh (nominal: 6.5 m from $Hb = 75$ m).

The annual energy production in the base configuration is:

$$ATEP = NAP \times Tfa = Q_{t_{ann}} Hn k \eta \times Tfa$$

$$ATEP = 9.81 \times 68.5 \times 835.73 \times 0.85 \times 7500 / 10^6 = 3580.19 \text{ GWh/year}$$

Table 10 shows sensitivity variation parameters on ATEP.

Variant ranking robustness

The relative ranking ($V2 > V3 > V1 > V4$ in energy; $V2 > V4 > V1 > V3$ in capacity factor) is preserved across all single-parameter sensitivity tests. This confirms that V2 is the robustly optimal variant over the plausible parameter range.

Table 10. Sensitivity variation.

	Sensitivity variation			Impacts
Sensitivity to net head (± 5 m around nominal 68.5 m)	$Hn = 63.5$ m \rightarrow ATEP = 3318.86 GWh	$Hn = 68.5$ m \rightarrow ATEP = 3580.19 GWh	$Hn = 73.5$ m \rightarrow ATEP = 3841.51 GWh	± 5 m head change produces $\pm 7.3\%$ energy variation.
Sensitivity to overall efficiency η ($\pm 5\%$ around nominal 85%)	$\eta = 80\%$ \rightarrow ATEP = 3369.59 GWh	$\eta = 85\%$ \rightarrow ATEP = 3580.19 GWh	$\eta = 90\%$ \rightarrow ATEP = 3790.79 GWh	efficiency has a strictly linear effect and $\pm 5.9\%$ energy variation
Sensitivity to head losses Δh	$\Delta h = 5.0$ m ($Hn=70.0$ m) \rightarrow ATEP = 3658.58 GWh	$\Delta h = 6.5$ m ($Hn=68.5$ m) \rightarrow ATEP = 3580.19 GWh (reference)	$\Delta h = 8.0$ m ($Hn=67.0$ m) \rightarrow ATEP = 3502 GWh	head losses have a moderate effect ($\pm 2.2\%$ per ± 1.5 m), smaller than efficiency

4. Discussion

The results obtained confirm the direct linear relationship between the hydrodynamic parameters of the Kouilou-Niari River and the energy production capacity of the Sounda Gorges power plant. This linearity, predicted by the fundamental equation $P = \rho g H n Q \eta$, is verified for all the hydrological regimes analyzed [9] [10] [12]. The proportionality coefficient k , which allows rapid estimation of the available power for any given flow rate, varies according to the net head height: $k = 0.542$ MW/(m³/s) for $Hn = 65$ m and $k = 0.570$ MW/(m³/s) for $Hn = 68.5$ m.

The flood/low-water ratio of 2.39 indicates strong seasonal variability in flows, which requires dynamic management of electricity production. During the flood period, the plant can provide 592.15 MW, enabling it to meet peak demand and export the surplus to neighboring countries via the Central African Power Pool. During the low-water period, the reduced power of 247.78 MW requires either supplementary production from other sources or rigorous demand management.

5. Conclusions

This study has modeled the hydrodynamic parameters of the Kouilou-Niari River and evaluated the energy efficiency of the Sounda Gorges hydroelectric power plant in Congo-Brazzaville. The analysis of 62 years of hydrological data (1952-2013) reveals a hydrological regime strongly influenced by regional rainfall, with an average annual flow rate of 928.53 m³/s exhibiting strong seasonal variability.

The results confirm the linear relationship between flow rates and energy production capacity. For a net head of 68.5 m and overall efficiency of 85%, the plant can generate electrical power of 592.15 MW during the flood period (October-May) and 247.78 MW during the low-water period (June-September), with an average annual power of 477.36 MW and total production of 4293.8 GWh/year (including 3580.19 GWh/year effective).

Additionally, the four variants proposed for the Sounda Gorges hydroelectric development have demonstrated good performance for optimal sizing. Variant 2 (4 Francis turbines, $Hn = 68.5$ m) offers the best performance: 778.08 MW in-

stalled, 89.7% efficiency, 4352.45 GWh/year production with 64.7 % capacity factor. Variant 4 (5 Francis turbines, $Hn = 65$ m) constitutes a viable economic alternative: 728.80 MW installed, 3913.66 GWh/year production.

These performances, consistent with international estimates (450 - 600 MW), position the Sounda Gorges power plant as a strategic asset for Congo's energy development and the Central African Power Pool, contributing to energy security, industrialization, and socio-economic development of the sub-region.

The simple interdependence laws obtained between characteristic parameters (flow rate, head, power) constitute practical tools for operational planning and optimal plant management. These results open promising perspectives for exploiting the hydraulic resources of the Kouilou-Niari River and, more broadly, for valorizing the hydroelectric potential of Central Africa.

This article thus opens an even broader horizon on the exploitation of hydraulic energies, particularly those that the river can provide for the construction of a hydroelectric power plant.

Acknowledgments

The authors express their gratitude to the Energie Electrique du Congo (E²C) company for access to technical pre-feasibility study data for the Sounda Gorges hydroelectric power plant project and to the ISTA-Kinshasa laboratory.

Conflicts of Interest

The authors declare no conflicts of interest regarding the publication of this paper.

References

- [1] Ministère de l'Energie et de l'Hydraulique, ANER (2013) Rapport national pour la formulation et la rédaction du livre Blanc de Politique Régionale pour "l'accès aux Services Energétiques dans les pays de la CEEAC-CEMAC intégrant les énergies renouvelables et l'efficacité énergétique et contribuant à la lutte contre la pauvreté". 28 p.
https://rise.esmap.org/sites/default/files/library/congo.-rep./Electricity%20Access/Congo_ANER%20Rapport%20National-RAGA_FR_2013.pdf
- [2] Cunge, J.A., Holly, F.M. and Verwey, A. (1980) Practical Aspects of Computational River Hydraulics. Pitman Publishing, 420 p.
- [3] Prancou, J. (1959) The Sounda Hydro-Electric on the Kouilou-Niari in the Development of Middle Congo. Technical Report, Ministry of Public Works, Brazzaville, Republic of Congo.
<https://www.shf-lhb.org/articles/lhb/pdf/1959/06/lhb1959046.pdf>
- [4] World Bank Group Archives (1958) Kouilou Hydro Electric and Industrial Complex Project, Pointe-Noire, Middle Congo. World Bank, Technical Report No. WB-AF-1958-KHE.
<https://thedocs.worldbank.org/en/doc/867421505836493986-0240021958/original/WorldBankGroupArchivesFolder1633883.pdf>
- [5] Ngoma Mvoundou, C. (2022) Modelisation Pluie-Debit dans le Bassin Kouilou-Niari.

- Ph.D. Thesis, Marien Ngouabi University.
- [6] Mvoundou, C.N., Tathy, C., Obami-Ondon, H., Moukoko, G.B.M. and Niere, R.R. (2022) Calibration and Validation of the GR2M Hydrologic Model in the Kouilou-Niari Basin in Southwestern Congo-Brazzaville. *Open Journal of Modern Hydrology*, **12**, 109-124. <https://doi.org/10.4236/ojmh.2022.123007>
 - [7] Chow, V.T., Maidment, D.R. and Mays, L.W. (1988) Applied Hydrology. McGraw-Hill, 149-175.
 - [8] Plaut, E. (2016) Fluid Mechanics. Lecture Notes, 2nd Year Course, Ecole des Mines de Nancy, Nancy, France, 2016. <http://emmanuelplaut.perso.univ-lorraine.fr/mf/pol.pdf>
 - [9] Hockney, R. and Eastwood, J. (1988). Computer Simulation Using Particles. Taylor & Francis, 265-301. <https://doi.org/10.1201/9781439822050>
 - [10] Mfenge, C.N., Mobonda, F.L., Moukengue, L.N., Tathy, C. and Ndiakama, G.E. (2023) Analysis of the Mechanical System Transforming Convertible Kinetic Energy into Electrical Energy in the Inga 2 Hydroelectric Power Plant. *World Journal of Advanced Research and Reviews*, **18**, 167-179. <https://doi.org/10.30574/wjarr.2023.18.2.0693>
 - [11] WMO (World Meteorological Organization) (2008) Guide to Hydrological Practices, Volume I: Hydrology from Measurement to Hydrological Information, 6th ed. WMO, 296 p. https://unstats.un.org/unsd/envaccounting/waterGuidelines/Material/WMO_Guide_168_Vol_I_en_hydrological_practices.pdf
 - [12] Hothersall, R. (2004) Hydrodynamic Design Guide for Small Francis and Propeller Turbines. 165 p. <https://downloads.unido.org/ot/47/88/4788275/20001-23096.pdf>
 - [13] Poff, N.L., Allan, J.D., Bain, M.B., Karr, J.R., Prestegard, K.L., Richter, B.D., *et al.* (1997) The Natural Flow Regime: A Paradigm for River Conservation and Restoration. *BioScience*, **47**, 769-784. <https://doi.org/10.2307/1313099>
 - [14] International Electrotechnical Commission (IEC) (2019) IEC 60193:2019—Hydraulic Turbines, Storage Pumps and Pump-Turbines—Model Acceptance Tests, 3rd ed. IEC.
 - [15] Warnick, C.C. (1984) Hydropower Engineering. Prentice-Hall, 85-99.
 - [16] Mishra, S., Singal, S.K. and Khatod, D.K. (2011) Optimal Installation of Small Hydropower Plant—A Review. *Renewable and Sustainable Energy Reviews*, **15**, 3862-3869. <https://doi.org/10.1016/j.rser.2011.07.008>
 - [17] Alligné, S., Béguin, A., Nicolet, C., *et al.*, (2025) Feasibility Study and Equipment Selection for the Rwanguba Hydropower Plant in Isolated Operation. https://hdynamics.ch/wp-content/uploads/2025/12/HYDRO2025_Thessaloniki_Alligne_Rwanguba_stability.pdf
 - [18] Mulu, B., Jonsson, P.P. and Cervantes, J. (2012) Experimental Investigation of a Kaplan Turbine Model under Steady-State and Transient Conditions. *Renewable Energy*, **46**, 55-63.
 - [19] Labadie, J.W. (2004) Optimal Operation of Multireservoir Systems: State-Of-The-Art Review. *Journal of Water Resources Planning and Management*, **130**, 93-111. [https://doi.org/10.1061/\(asce\)0733-9496\(2004\)130:2\(93\)](https://doi.org/10.1061/(asce)0733-9496(2004)130:2(93))
 - [20] Fraenkel, P., Parish, O., Bolkalders, V., Harvey, A., Brown, A. and Edwards, R. (1991) Micro-Hydro Power: A Guide for Development Workers. Intermediate Technology Publications, 78-102.

- [21] Picollier, G. and Girault, P. (1986) Économie et performance des petites turbines. Société hydrotechnique de France, 11p.
<https://www.tandfonline.com/doi/epdf/10.1051/lhb/1986006>

Appendix 1: Flow Rates (in m³/s) Prelevé in Kouilou-Niari River from 1952 to 2013 [5]

years	Months											
	Jan.	Feb.	Mar.	April	May	June	July	Aug.	Sept.	Oct.	Nov.	Dec.
1952	1120.3	1165.7	1299.7	1466.5	1457.8	727.8	634.0	492.0	420.0	482.0	1621.0	1826.0
1953	1243.0	1443.0	1821.0	2363.0	2682.0	1366.0	738.0	458.0	410.0	418.0	1008.0	1344.0
1954	761.0	930.0	1191.0	1484.0	1316.0	597.0	395.0	317.0	269.0	467.0	913.0	955.0
1955	1207.0	769.0	979.0	1845.0	2273.0	1283.0	656.0	494.0	399.0	499.0	1380.0	1787.0
1956	1293.0	1095.0	683.0	936.0	1198.0	519.0	397.0	328.0	283.0	347.0	700.0	1221.0
1957	1175.0	1202.0	1692.0	1551.0	1373.0	747.0	493.0	388.0	327.0	320.0	774.0	1328.0
1958	742.0	499.0	550.0	662.0	594.0	348.0	280.0	262.0	242.0	270.0	581.0	847.0
1959	829.0	1320.0	1195.0	1484.0	1320.0	549.0	398.0	328.0	288.0	381.0	998.0	1443.0
1960	757.0	1214.0	1221.0	1424.0	1553.0	712.0	468.0	372.0	329.0	424.0	1600.0	1629.0
1961	1889.0	2055.0	2620.0	2046.0	1870.0	844.0	616.0	460.0	432.0	843.0	1959.0	2298.0
1962	1476.0	1667.0	1786.0	1958.0	1838.0	834.0	592.0	467.0	394.0	532.0	875.0	1393.0
1963	1210.0	1207.0	1373.0	1570.0	1563.0	688.0	500.0	392.0	333.0	342.0	904.0	1120.0
1964	1390.0	975.0	1010.0	1830.0	2040.0	983.0	610.0	452.0	386.0	379.0	1090.0	1790.0
1965	1100.0	1170.0	1210.0	1610.0	1730.0	830.0	550.0	445.0	386.0	427.0	755.0	997.0
1966	1130.0	1380.0	1480.0	2100.0	2470.0	946.0	624.0	479.0	392.0	480.0	1270.0	1060.0
1967	1158.0	1601.0	2077.0	1211.0	1195.0	663.0	487.0	404.0	361.0	528.0	1288.0	1086.0
1968	975.0	828.0	1080.0	1370.0	1210.0	553.0	407.0	335.0	277.0	337.0	750.0	1118.0
1969	998.0	848.0	1104.0	1375.0	1229.0	546.0	405.0	337.0	274.0	328.0	874.0	1272.0
1970	895.0	1385.0	1860.0	1986.0	1800.0	795.0	526.0	420.0	372.0	407.0	1450.0	1600.0
1971	891.0	862.0	972.0	999.0	1090.0	566.0	396.0	322.0	279.0	335.0	1040.0	954.0
1972	815.0	637.0	557.0	968.0	1100.0	518.0	365.0	290.0	259.0	290.0	1010.0	1210.0
1973	1110.0	1000.0	878.0	1480.0	2080.0	1320.0	569.0	428.0	372.0	469.0	1280.0	1250.0
1974	1290.0	1540.0	1410.0	1540.0	1220.0	663.0	477.0	398.0	345.0	347.0	820.0	829.0
1975	997.0	1270.0	1370.0	1410.0	1130.0	658.0	465.0	366.0	316.0	393.0	1170.0	1230.0
1976	1150.0	1320.0	1420.0	1370.0	1250.0	612.0	440.0	369.0	330.0	319.0	626.0	1220.0
1977	1340.0	1250.0	1840.0	1540.0	1260.0	897.0	543.0	437.0	363.0	449.0	1160.0	1590.0
1978	1050.0	773.0	577.0	536.0	573.0	353.0	285.0	235.0	201.0	206.0	825.0	998.0
1979	1190.0	1110.0	1200.0	1490.0	1700.0	831.0	526.0	396.0	354.0	339.0	558.0	943.0
1980	1280.0	1210.0	958.0	1210.0	1480.0	642.0	445.0	366.0	325.0	346.0	852.0	1200.0
1981	1120.0	1190.0	1700.0	1400.0	829.0	488.0	382.0	315.0	285.0	464.0	994.0	1610.0
1982	1149.0	1221.0	1176.0	1247.0	769.0	483.0	390.0	312.0	261.0	275.0	808.0	1020.0
1983	3265.5	3303.5	2643.6	2140.0	1552.8	1212.9	998.0	864.7	776.9	895.2	1327.0	1126.8
1984	1395.5	1498.8	1574.8	1357.2	1079.1	788.8	628.5	578.3	560.4	713.2	1294.0	991.1
1985	961.1	999.9	1042.7	1272.6	973.4	708.0	566.7	506.1	464.3	616.0	1100.1	1002.7
1986	1101.3	1373.4	1286.5	1350.3	1137.9	778.3	622.6	552.4	502.4	532.0	708.2	822.1
1987	668.8	984.4	1153.1	1103.8	861.7	618.9	496.9	465.6	437.8	467.5	939.7	1115.3

Continued

1988	916.4	1154.2	1093.8	1044.5	842.9	610.5	494.4	442.5	404.5	530.0	820.0	852.5
1989	778.2	1247.7	1039.5	1147.3	1172.1	753.9	593.0	526.3	514.5	716.6	1143.8	1136.6
1990	1053.4	1201.1	1440.5	1189.5	915.0	687.1	562.0	503.6	455.1	769.8	1227.4	1150.1
1991	1282.9	1359.8	1258.8	1589.0	1214.1	826.3	659.5	578.6	519.5	480.5	793.0	685.7
1992	665.4	990.7	1053.8	922.1	754.2	560.3	460.1	408.6	377.3	352.3	703.6	747.6
1993	839.6	917.5	824.9	927.9	610.3	485.1	398.2	356.3	326.6	411.9	629.2	692.9
1994	510.3	556.9	651.5	740.9	557.2	422.9	344.3	316.0	289.1	622.1	1357.7	1506.3
1995	1383.8	1503.2	1476.4	1432.0	977.9	751.8	615.1	553.4	502.1	685.8	1280.3	1091.0
1996	1030.8	1322.6	1509.5	1435.1	1019.9	757.9	621.0	543.1	493.1	549.8	975.2	778.4
1997	752.9	850.1	1017.9	963.9	815.4	593.9	478.4	422.1	385.6	611.0	873.9	1264.2
1998	1216.4	1199.1	1381.9	1091.0	904.2	660.6	531.2	472.5	476.6	752.0	1340.9	1326.2
1999	1066.9	1664.3	1287.9	1556.2	1251.7	864.5	678.2	598.4	558.1	553.3	1520.2	1921.7
2000	1302.2	1752.8	1374.0	1428.6	1441.5	919.2	727.3	637.2	594.7	744.3	1183.3	1222.0
2001	1297.5	1522.4	1353.4	1531.2	1055.0	770.1	627.0	546.7	495.3	460.9	589.5	567.8
2002	655.0	946.0	896.8	887.8	658.7	492.9	398.0	356.9	344.8	565.6	707.4	852.8
2003	793.9	937.3	995.2	1174.7	793.6	592.8	478.4	421.9	405.1	676.8	1030.4	1091.5
2004	1500.8	1463.4	1269.1	1222.5	763.2	630.2	523.5	468.6	422.6	560.3	1136.7	1177.2
2005	1221.8	1250.5	1176.9	1143.8	741.3	599.6	499.7	442.2	406.1	657.3	885.0	837.3
2006	824.9	1288.6	1249.1	1268.8	841.0	635.1	514.8	460.5	420.8	639.8	1651.9	1678.3
2007	1403.0	1515.4	1671.3	1533.4	1443.9	934.1	737.0	639.1	577.5	938.4	634.9	907.3
2008	949.5	1231.8	1104.5	1596.0	1178.9	801.3	636.4	570.2	523.4	838.7	1266.2	1292.4
2009	1222.7	1891.9	1619.9	1855.7	1344.1	923.3	740.0	643.4	577.8	795.0	1107.5	1363.1
2010	1592.8	1286.1	1709.9	1366.6	972.0	740.1	606.8	530.6	487.5	625.6	1259.9	1485.1
2011	1743.0	1800.3	1287.6	1583.1	989.3	772.1	631.5	554.5	499.7	806.9	1189.1	1040.8
2012	742.4	963.7	977.7	991.7	898.8	628.1	501.1	443.1	427.1	612.8	1084.8	1207.6
2013	1146.7	1393.9	1366.1	1453.4	994.6	733.6	594.8	527.0	472.7	650.2	848.2	1000.9

Appendix 2: Calculation Formulas

1. Average flow rate during the flood period for year i :

$$Q_{flood}(i) = (1/7) * \sum Q_{ij} \quad \text{for } j \in \{\text{Oct, Nov, Dec, Jan, Feb, Mar, Apr}\}$$

2. Average flow rate during the low-water period for year i :

$$Q_{low}(i) = (1/5) * \sum Q_{ij} \quad \text{for } j \in \{\text{May, June, July, Aug., Sept}\}$$

3. Average annual flow rate for year i :

$$Q_{ann}(i) = (1/12) * \sum Q_{ij} \quad \text{for } j = 1 \text{ to } 12$$

4. Average flow rate over the entire period :

$$Q_{moy} = (1/N) * \sum Q_i \quad \text{for } i = 1 \text{ to } N (N = 62 \text{ years})$$

5. Standard deviation (measure of variability)

$$\sigma = \sqrt{(1/(N-1)) * \sum (Q_i - Q_{moy})^2}$$